D3.4 Phytoplankton Size Class Product Documentation

This project has received funding from the European Union's Horizon 2020 research and innovation programme under grant agreement No 776348.

Project no.	776348
Project acronym:	CoastObs
Project title:	Commercial service platform for user-relevant coastal water monitoring services based on Earth Observation
Instrument:	H2020-EO-2017
Start date of project:	01.11.2017
Duration:	36 months
Deliverable title:	D3.4 Phytoplankton Size Class Product Documentation
Due date of deliverable:	Month 19

Organisation name of lead contractor for this deliverable: USTIR

Author list:

Name	Organisation
Caitlin Riddick	University of Stirling
Evangelos Spyrakos	University of Stirling
Peter Hunter	University of Stirling
Andrew Tyler	University of Stirling
Anne-Laure Barillé	Bio-littoral

Dissemination level		
PU	Public	X
CO	Confidential, restricted under conditions set out in Model Grant Agreement	
CI	Classified, information as referred to in Commission Decision 2001/844/EC	

This project has received funding from the European Union's Horizon 2020 research and innovation programme under grant agreement No 776348

History			
Version	**Date**	**Reason**	**Revised by**
01	20/05/2019	Initial Draft for review	Caitlin Riddick (USTIR)
02	21/05/2019	Internal Review	Evangelos Spyrakos (USTIR)
03	31/05/2019	Internal Review	Anne-Laure Barillé (Bio-littoral)
04	31/05/2019	Revised Draft for submission	Caitlin Riddick (USTIR)

Please cite as:

Riddick, C.A.L., Spyrakos, E.S., Hunter, P.D., Tyler, A.N., Barillé, A. (2019). D3.4 Phytoplankton Size Class Product Documentation. CoastObs Project.

This project has received funding from the European Union's Horizon 2020 research and innovation programme under grant agreement No 776348

CoastObs Project

CoastObs is an EU H2020 funded project that aims at using satellite remote sensing to monitor coastal water environments and to develop a user-relevant platform that can offer validated products to users including monitoring of seagrass and macroalgae, phytoplankton size classes, primary production, and harmful algae as well as higher level products such as indicators and integration with predictive models.

phytoplankton

seagrass

harmful algal blooms

primary production

To fulfil this mission, we are in dialogue with users from various sectors including dredging companies, aquaculture businesses, national monitoring institutes, among others, in order to create tailored products at highly reduced costs per user that stick to their requirements.

With the synergistic use of Sentinel-3 and Sentinel-2, CoastObs aims at contributing to the sustainability of the Copernicus program and assisting in implementing and further fine-tuning of European Water Quality related directive.

This project has received funding from the European Union's Horizon 2020 research and innovation programme under grant agreement No 776348

Partnership

Water Insight BV. (WI)

The University of Stirling (USTIR)

Consiglio Nazionale Delle Ricerche (CNR)

Universite de Nantes (UN)

HZ University of Applied Sciences (HZ)

Universidad de Vigo (UVIGO)

Bio-Littoral (BL)

Geonardo Environmental Technologies Ltd. (GEO)

This project has received funding from the European Union's Horizon 2020 research and innovation programme under grant agreement No 776348

TABLE OF CONTENTS

This project has received funding from the European Union's Horizon 2020 research and innovation programme under grant agreement No 776348

FIGURES

This project has received funding from the European Union's Horizon 2020 research and innovation programme under grant agreement No 776348

TABLES

This project has received funding from the European Union's Horizon 2020 research and innovation programme under grant agreement No 776348

1 Summary

Phytoplankton are typically classified into three size classes: pico- (<2 µm), nano- (2-20 µm) and micro-phytoplankton (>20 µm) (Sieburth et al., 1978). Phytoplankton size class (PSC) is therefore an indicator of cell size, and considered to reflect the ecological and biogeochemical functional role of the phytoplankton present in the water column (Sieburth et al., 1978; Irwin, 2006; Nair et al., 2008; Finkel et al. 2009; Marañón, 2015; Liu et al., 2018). Thus, it is important to be able to monitor PSCs, particularly in dynamic coastal waters where there are frequent changes in nutrients and phytoplankton community structure. A PSC product from earth observation (EO) is of importance to the CoastObs project users, in particular managers and aquaculture producers.

Thus, this deliverable provides the product documentation for the CoastObs PSC product, including model method, *in situ* model performance and satellite model performance. PSC models were tested using a historic dataset in the Ria de Vigo (Spain), and preliminary testing of these models using the 2018 field campaign data from the Adriatic (Italy) and Galician coastal waters (Spain) is presented. Models were forced with satellite data from MERIS, Sentinel-2 MSI and Sentinel-3 OLCI and re-tuned for each site. Future campaigns are planned for 2019 to validate the PSC models and tune the models for use in other sites (e.g. Wadden Sea and Eastern Scheldt, Netherlands). The PSC Sentinel-2 and -3 model validation results will be presented in the forthcoming Validation Report (D3.8).

This project has received funding from the European Union's Horizon 2020 research and innovation programme under grant agreement No 776348

2 Introduction

Phytoplankton are typically classified into three size classes: pico- (<2 µm), nano- (2-20 µm) and micro-phytoplankton (>20 µm) (Sieburth et al., 1978). Phytoplankton size class (PSC) is therefore an indicator of cell size, and considered to reflect the ecological and biogeochemical functional role of the phytoplankton present in the water column (Sieburth et al., 1978; Irwin, 2006; Nair et al., 2008; Finkel et al. 2009; Marañón, 2015; Liu et al., 2018). PSC is also related to the physiology of phytoplankton (Platt and Denman, 1976; Chisholm, 1992; Raven, 1998), the marine food web (Parsons and Lalli, 2002), fish production (Caddy et al., 1995), metabolic rates (Platt and Denman, 1977; 1978) and mussel growth and condition (Safi and Gibbs, 2003).

Thus, it is important to be able to monitor PSCs, particularly in dynamic coastal waters where there are frequent changes in nutrients and phytoplankton community structure. Coastal waters are also often the sites of marine aquaculture (or mariculture) where information on PSCs is of particular importance to managers and aquaculture producers. Many studies indicate that the minimum particle size for efficient bivalve retention is 4 µm (i.e. nano- and micro-phytoplankton are the preferred food source) (Muniz et al., 2019; Jørgensen, 1990; Møhlenberg and Riisgård, 1978; Riisgård, 1988). However, other studies have found that the contribution of pico- and nano-phytoplankton (<2.0 um) to mussel retention efficiency is non-negligible and should be taken into account (Sonier et al., 2016).

Furthermore, phytoplankton size can impact the optical properties of the water; for example, light absorption by large cells is influenced by intracellular shading, or the so-called pigment packaging effect (Bricaud et al., 1995). This in turn influences the reflectance signature retrieved by satellite data and thus impacts the ability to use earth observation for ocean colour monitoring.

Earth observation (EO) provides the opportunity to monitor the frequent changes in phytoplankton abundance in coastal waters, using the photosynthetic pigment chlorophyll-*a* (Chl-*a*) as a proxy. In turn, there are several models to derive the PSCs from either Chl-*a* or spectral absorption data or both, and these will be described in further detail below.

The PSC models were tested as part of the CoastObs project using historic datasets as well as preliminary testing of these models using the 2018 field campaign data from the Adriatic (Italy) and Galician coastal waters (Spain). Models were then forced with satellite data from Sentinel-2 MSI and Sentinel-3 OLCI and calibrated for the two sites. Future campaigns are planned for 2019 to validate the PSC models and extend the models for use in other sites (e.g. Wadden Sea and Eastern Scheldt, Netherlands).

This project has received funding from the European Union's Horizon 2020 research and innovation programme under grant agreement No 776348

3 Phytoplankton Size Class models

3.1 Pigment-based models

Uitz et al. (2006) developed a model based on high performance liquid chromatography (HPLC) data, which infers the vertical distribution of the three PSCs. This method uses a Diagnostic Pigment Analysis (DPA; Vidussi et al. 2001; revised by Uitz et al., 2006) which uses marker pigments to identify major taxa. The taxa are then characterised into size classes, as in Table 1.

However, the pigment approach does have limitations, as HPLC is not a direct measurement of phytoplankton size class. For example, marker pigments are often shared between several phytoplankton taxa, thus assumptions have to be made about the ratio of Chl-*a* to the accessory pigments.

Table 1 - Taxa, marker pigment and size class (From Hirata et al., 2008)

Taxonomic group	Marker pigments (abbreviation)	Size class
Diatoms	Fucoxanthin (Fuc)	Micro
Dinoflagellates	Peridinin (Per); also Fuc	Micro
Flagellates		
Prymnesiophytes	19′-Hexanoyloxyfucoxanthin (Hex)	Nano
Chrysophytes	19′-butanoyloxyfucoxanthin (But)	Nano
Cryptophytes	Alloxanthin (Allo)	Nano
Chlorophytes	Chlorophyll b (Chlb)	Nano
Pico-flagellates or	(Hex, But, Allo, Chlb)	Pico
Pico-eukaryotes		
Cyanobacteria (prokaryotes; prok)		Pico
Synechococcus spp.	Zeaxanthin (Zea)	Pico
Prochlorococcus spp.	Zeaxanthin (Zea)+DVChlb	Pico

Diagnostic pigments (DP) = 0.6Allo+0.35But+1.01Chlb+1.41Fuc+1.27Hex+1.41Per+0.86Zea.
Micro (M)=1.41(Fuc+Per)/DP.
Nano (N)=(0.6Allo+0.35But+1.27Hex+1.01Chlb)/DP.
Prokaryotes (Cyanobacteria)=0.86Zea/DP.
PE = pico-eukaryotes (size <2 μm, Chla <0.25 mg m^{-3}).
Pico (P)=Prok+PE.

3.2 Spectral absorption-based models

Hirata et al. (2008) derived relationships between phytoplankton optical properties and PSCs. More specifically, this approach uses a relationship between phytoplankton absorption at 443 nm ($a_{ph}(443)$) to the absorption spectral slope over 443-510 nm (S). This is a threshold based method, which classifies the three phytoplankton populations as follows, as in Liu et al (2018):

This project has received funding from the European Union's Horizon 2020 research and innovation programme under grant agreement No 776348

pico-phytoplankton $a_{ph}(443)<0.023$ m^{-1}; nano-phytoplankton $0.023<=a_{ph}(443)<0.069$ m^{-1}; micro-phytoplankton, $a_{ph}(443)>=0.069$ m^{-1}.

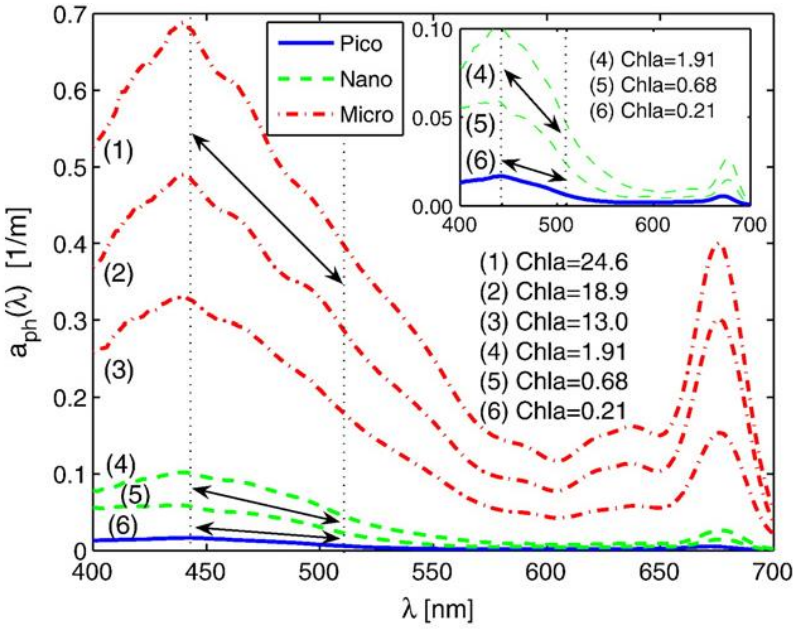

Figure 1 - Phytoplankton absorption spectra for a range of Chla for pico-, nano- and micro-phytoplankton with decreasing slope from high to low aph(λ) and Chla (from Hirata et al. 2008)

3.3 Ecological based models

The ecological based model developed by Barnes et al. (2011) predicts the size composition of the phytoplankton community using Chl-*a* and sea surface temperature (SST). More specifically, empirical relationships are established between phytoplankton biomass and Chl-*a* or SST. The biomass in each group (pico-, nano- and micro-phytoplankton) is then determined with these relationships by integrating the biomass within cell mass ranges.

3.4 Abundance-based models

Most recently, a three-component model was developed by Brewin et al (2010), which calculates the fractional contributions of three PSCs from satellite Chl-*a* data over open ocean waters. This was conceptually based on the 2-component models of Sathyendranath et al (2001) and Devred et al. (2006), which assume that small cells dominate at low Chl-*a* concentrations and large cells at higher Chl-*a* concentrations (Figure 1). The model assumes small phytoplankton are incapable of growing beyond a particular Chl-*a* concentration, as there is an upper limit imposed from bottom-up (e.g. nutrient control) and top-down (e.g. grazing)

This project has received funding from the European Union's Horizon 2020 research and innovation programme under grant agreement No 776348

processes. The Brewin et al (2010) PSC model was validated in ocean waters using the Atlantic Meridional Transect (AMT) pigment data.

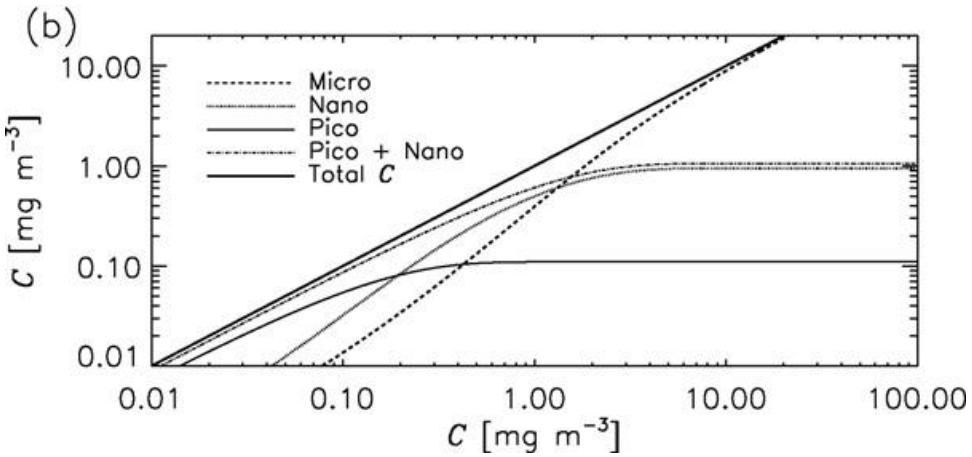

Figure 2 – Changes in chlorophyll-a of the three size classes in the model (logy-axis) as a function of the total chlorophyll-a concentration (log x-axis) (from Brewin et al., 2010).

The Brewin et al (2010) model attributes a fraction of the concentration of total Chl-*a* (*C*) to each PSC, such that:

$$C = C_1 + C_2 + C_3 \quad (\text{mg m}^{-3}) \qquad (1)$$

where:

C_1 = Chl-*a* <2 µm (pico-phytoplankton)

C_2 = Chl-*a* 2-20 µm (nano-phytoplankton)

C_3 = Chl-*a* >20 µm (micro-phytoplankton)

Both the smallest size class (C_1) and the combined two smallest size classes ($C_{1,2}$) are modelled according to an exponential function as follows:

$$C_1 = C_1^m[1 - \exp(-S_1 C)] \quad (\text{mg m}^{-3}) \qquad (2)$$

$$C_{1,2} = C_{1,2}^m\left[1 - \exp(-S_{1,2} C)\right] \quad (\text{mg m}^{-3}) \qquad (3)$$

Where C_1^m and $C_{1,2}^m$ are the asymptotic maximum values for C_1 and $C_{1,2}$, and S_1 and $S_{1,2}$ are the the initial slopes, respectively. Equations (2) and (3) were fitted using a standard nonlinear least squares method (Levenberg-Marquardt, R `minipack.lm` package).

Once C1 and C1,2 are known, C2 can be calculated as:

$$C_2 = C_{1,2} - C_1 \quad (\text{mg m}^{-3}) \qquad (4)$$

And the largest size class, C_3, can then be derived from total Chl-*a*, C, as:

This project has received funding from the European Union's Horizon 2020 research and innovation programme under grant agreement No 776348

$$C_3 = C - C_{1,2} \quad (\text{mg m}^{-3}) \qquad (5)$$

Subsequently, the Brewin et al. (2010) three-component model has been modified using a sea surface temperature (SST) dependent parameterisation (Brewin et al., 2017). This partitioned dataset into <15°C and ≥15°C for separate fitting and parameterisation by SST, however there was only marginal difference in using the SST-dependent parameterisation and the Brewin et al. (2010) model (Figure 3).

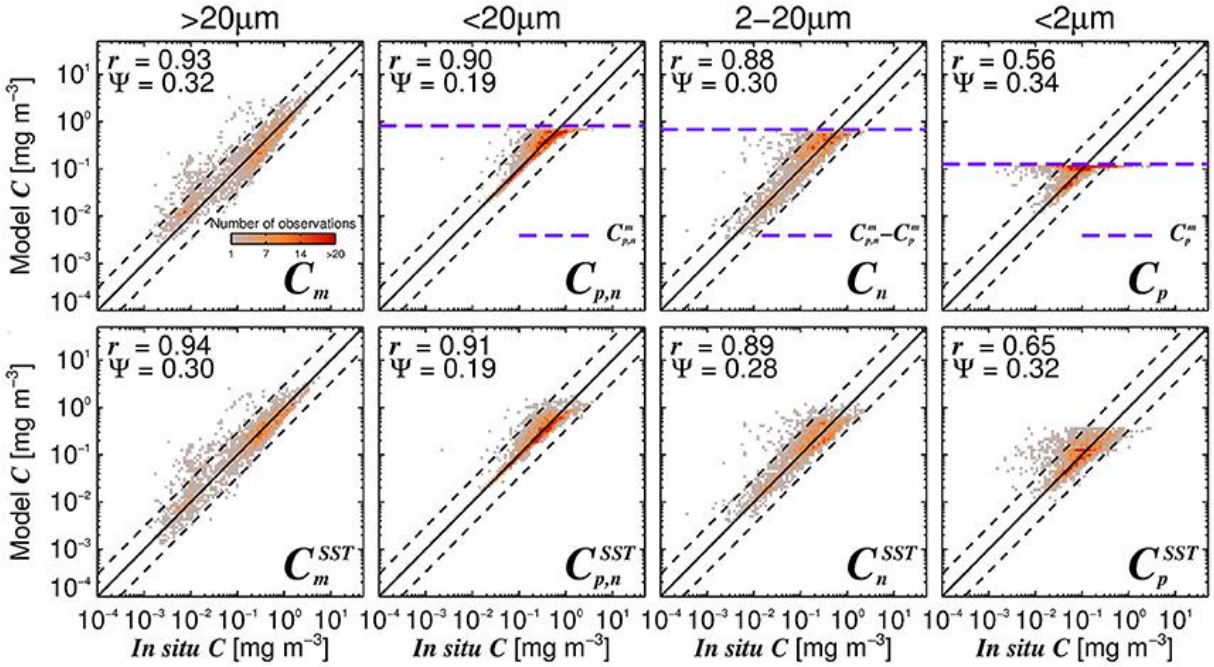

Figure 3 – Modelled size fractionated Chl-a plotted againsg in situ size fractionated Chl-a for the Brewin et al. (2010) model (top-row) and the SST-dependent parameterisation (bottom row) (taken from Brewin et al., 2017).

4 Initial retuning and validation

4.1 Historic Dataset

Fractionated Chl-*a* data from Vigo was obtained for 2006-2008 for two size classes: <2.7 µm and >2.7 µm (INTECMAR Oceanographic Annual Report, http://www.intecmar.gal/Informacion/fito/Anuarios/Default.aspx?sm=b4). These data were used to test a modified 2-class abundance-based model, using the Brewin et al (2010) approach, which uses total Chl-a data to model fractionated Chl-a. This was the available historic dataset, therefore other PSC models could not be tested on these data.

This project has received funding from the European Union's Horizon 2020 research and innovation programme under grant agreement No 776348

4.1.1 Methods

4.1.1.1 In situ

Surface (0-5 m) water samples were collected on a weekly basis by INTECMAR from Ria de Vigo and the Estuary of Baiona, Spain at the stations indicated in Figure 4.

For the analysis of Chl-*a*, 10 ml of seawater was filtered onto glass fibre filters. To obtain fractionated Chl-*a*, samples were filtered first on a 2.7 µm filter to represent the nano- and micro-phytoplankton fraction (>2.7 µm). The filtrate was subsequently filtered again on a 0.7 µm filter for collection of pico-phytoplankton Chl-*a* fraction (0.7-2.7 µm).

Chl-*a* was then extracted in acetone chilled to 90% for at least 14 hours. Extracts were then analysed by spectrofluorimetry by means of a trichromatic equation, using the Neveaux & Panouse method (1987) with modifications of Zapata et al. (1987).

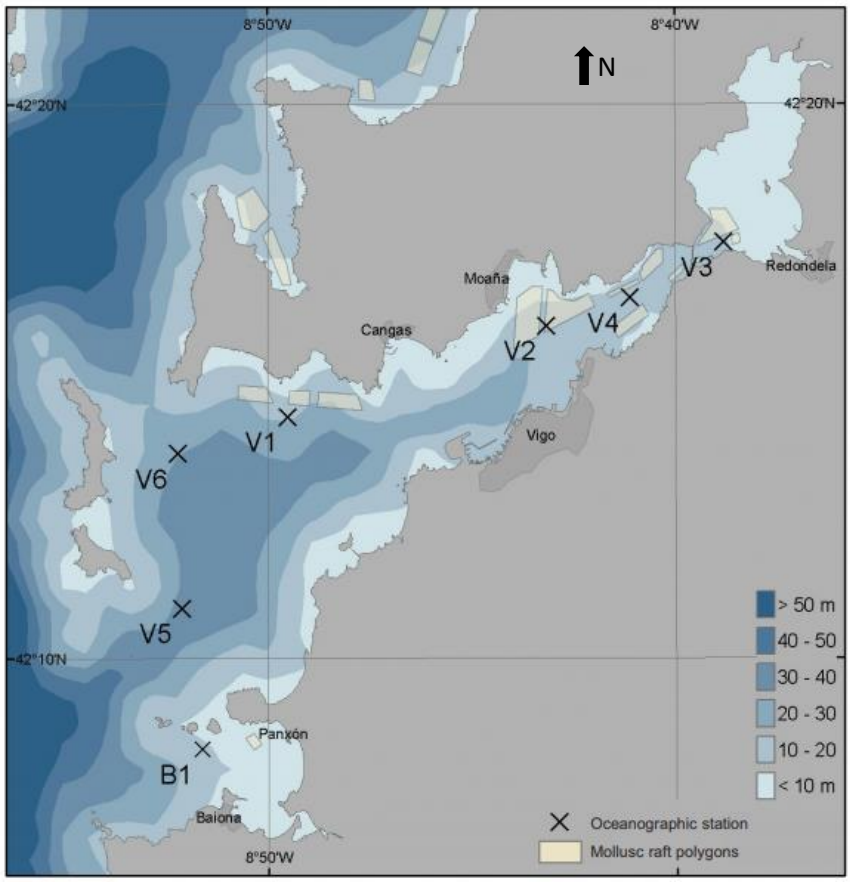

Figure 4 - Historic sampling locations in Ria de Vigo (from INTECEMAR Oceanographic Annual Report, 2006).

This project has received funding from the European Union's Horizon 2020 research and innovation programme under grant agreement No 776348

For the historic dataset in ria de Vigo, pico-phytoplankton Chl-*a* (0.7-2.7 µm) ranged from 0-17 mg m^{-3} (mean = 0.11 ± 0.55 mg m^{-3}) and nano- + microphytoplankton Chl-*a* (>2.7 µm) ranged from 0-29.4 mg m^{-3} (mean = 1.51 ± 1.98 mg m^{-3}).

4.1.1.2 Model

Using the historic dataset, a modified 2-class model from the Brewin et al (2010) abundance-based approach was applied. Given the dataset available, C was a sum of the two fractions:

$$C = C_1 + C_{2,3} \quad (\text{mg m}^{-3}) \quad (6)$$

where:

C_1 = Chl-*a* 0.7-2.7 µm (pico-phytoplankton)

$C_{2,3}$ = Chl-*a* >2.7 µm (nano- and micro-phytoplankton)

As in Brewin et al (2010), a model for the pico-phytoplankton Chl-*a* component (C_1) followed an nonlinear asymptotic function:

$$C_1 = C_1^m[1 - \exp(-S_1 C)] \quad (7)$$

Where C_1^m is the asymptotic maximum value for C_1, and S_1 is the the initial slope. The combined nano- and micro-phytoplankton class Chl-*a* component ($C_{2,3}$) was then calculated by subtraction from total Chlorophyll-*a* (C):

$$C_{2,3} = C - C_1 \quad (8)$$

The rationale behind this model is that the fractions of Chl-*a* in the Vigo historic dataset followed a similar pattern to that observed by Brewin et al (2010) in ocean waters. In the Vigo 2006-2008 dataset, the fraction of picoplankton (F_1) followed a decreasing pattern with increasing total Chl-*a* (C), while the fraction of nano + micro-plankton ($C_{2,3}$) increased with increasing C (Figure 5). This is similar to the trends found by Brewin et al (2010) in ocean waters for F_1 (decreasing), while the Vigo 2006-2008 pattern for $F_{2,3}$ followed that observed by Brewin et al (2010) for micro-phytoplankton only (F_3; increasing) (Figure 6).

This project has received funding from the European Union's Horizon 2020 research and innovation programme under grant agreement No 776348

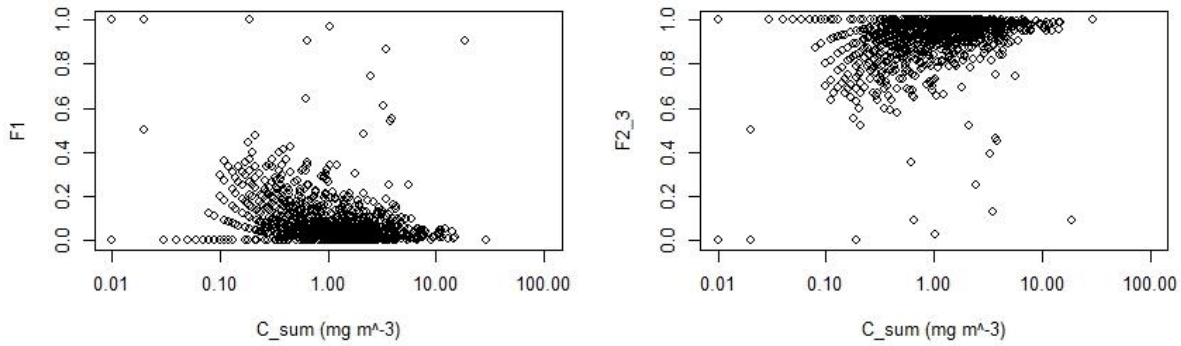

Figure 5 – Fraction of pico-phytoplankton (F1) and nano- + micro-phytoplankton (F2_3) as a function of the summed Chl-a (C_sum) in the ria de Vigo.

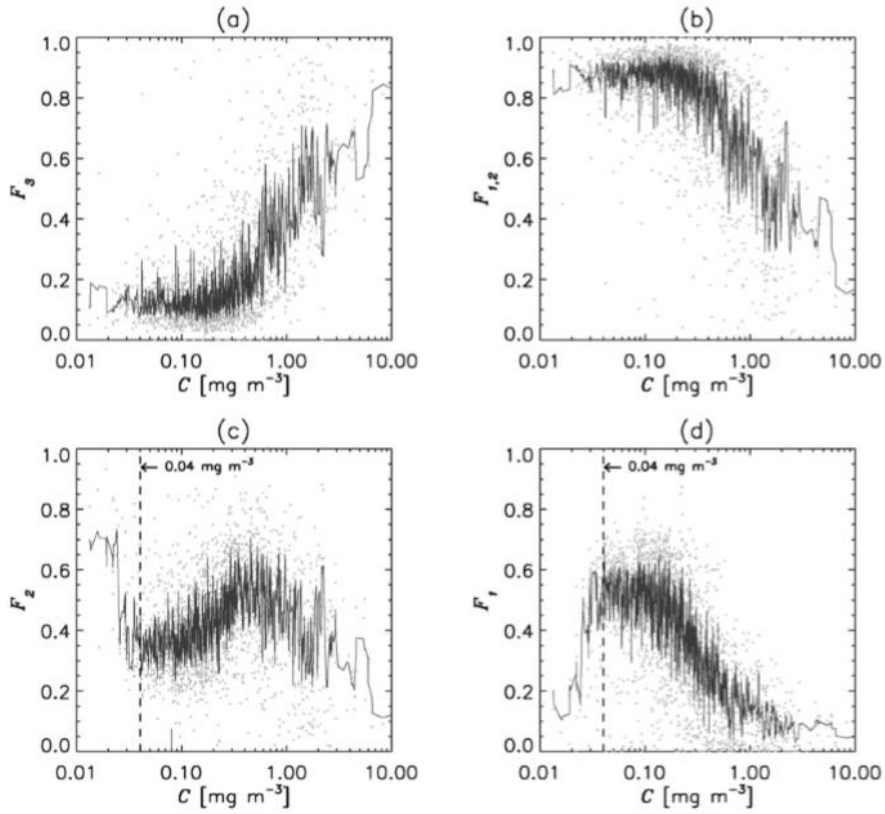

Figure 6 – Fraction of microplankton (a), combined nano- and picoplankton (b), nanoplankton (c), and picoplankton (d) as a function of chlorophyll-a for ocean waters (from Brewin et al., 2010).

4.1.2 Performance of *in situ* model

4.1.2.1 Retuned model parameters for C_1 (Pico-phytoplankton)

The model for C_1 is shown below, indicating nonlinear asymptotic function with high significance ($p<0.001$; Figure 7). The model coefficients are shown in Table 1.

This project has received funding from the European Union's Horizon 2020 research and innovation programme under grant agreement No 776348

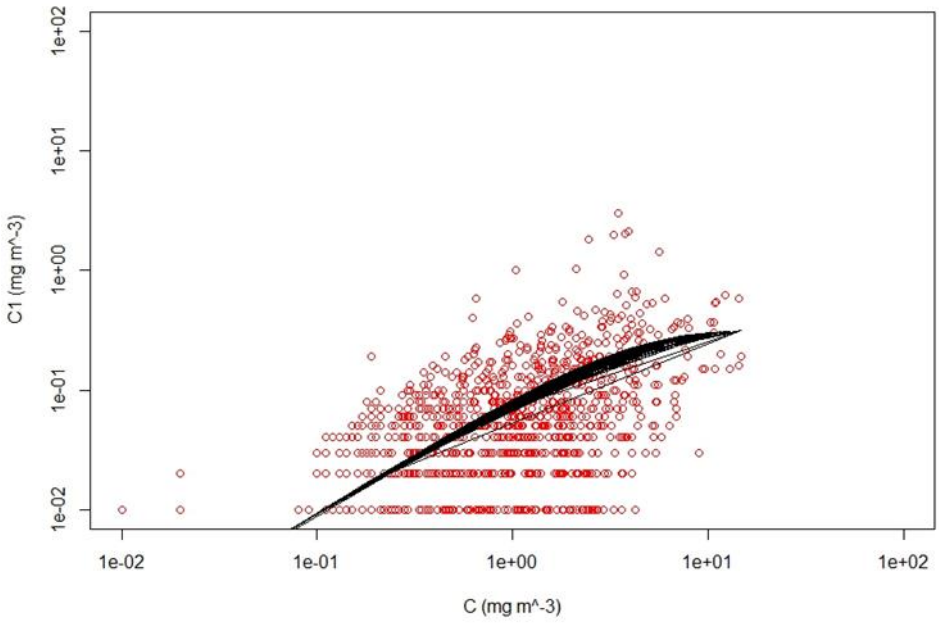

Figure 7 – In situ exponential model for fraction of Chl-a attributed to pico-phytoplankton (C1) as a function of total Chl-a (C) ($C_1 = C_1^m[1 - exp(-S_1C)]$, p<0.001).

Table 2 - Retuning coefficients for Vigo 2006-2008 2-class PSC model

Phytoplankton fraction	Coefficient	Value
Pico-phytoplankton (C_1)	C_1^m	0.3165
	S_1	0.3003

4.1.2.2 Model validation

The model was applied to *in situ* total Chl-*a* (C) to derive a modelled C_1 (and from this, a modelled $C_{2,3}$). The model validation plots are shown in Figure 8 and indicate good agreement between modelled and measured values, particularly for nano- + micro-phytoplankton ($C_{2,3}$) (R^2 = 0.9931). This is unsurprising as there are frequently values of C_1=0, i.e. pico-phytoplankton are absent ~ 10% of the time in the Vigo 2006-2008 dataset (not shown on log plot in Figure 8a). If the zeroes are removed from the *in situ* C_1 dataset, the model performs slightly better (R^2=0.0943).

This project has received funding from the European Union's Horizon 2020 research and innovation programme under grant agreement No 776348

(a)

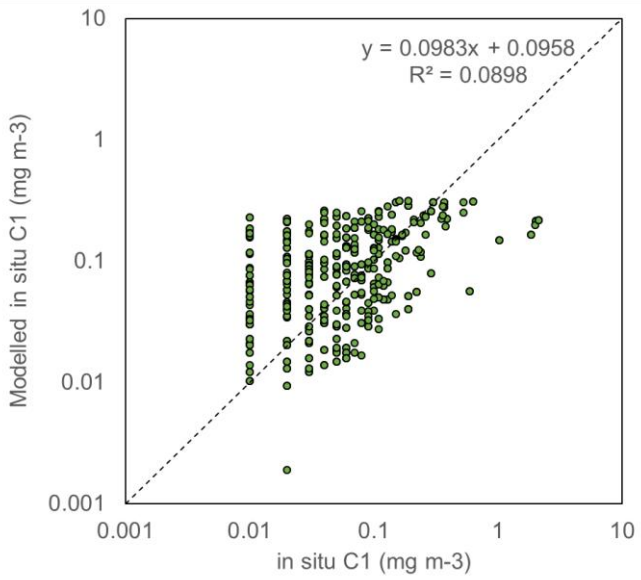

(b)

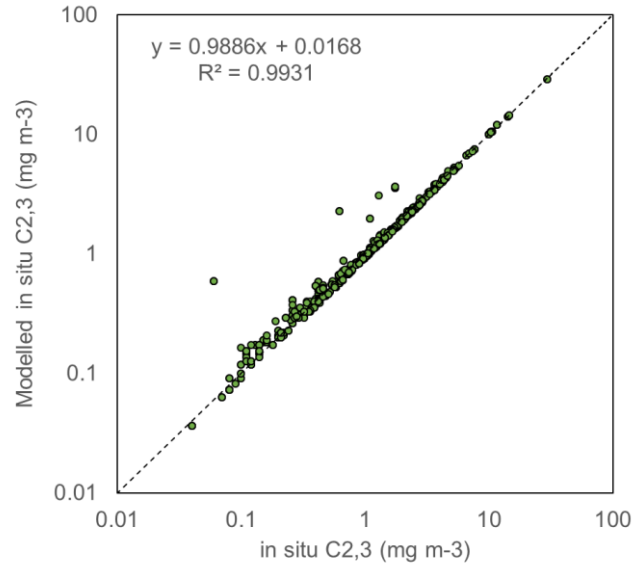

Figure 8 – In situ model performance for (a) pico-phytoplankton (C_1) and (b) nano- + micro-phytoplankton ($C_{2,3}$).

This project has received funding from the European Union's Horizon 2020 research and innovation programme under grant agreement No 776348

4.1.3 Performance of satellite model

Following validation of the *in situ* model performance, the model was then forced with satellite data from MERIS (as this was active during 2006-2008).

MERIS full resolution (FR) level-2 data were acquired from the MERCI website (https://merisfrs-merci-ds.eo.esa.int). Cloud, land and coastline pixels were removed using the L2 masks. Matchups with *in situ* data were extracted as single pixels +/-1 day of the satellite overpass. Chl-*a* was derived from MERIS Full resolution Level 2 (FR L2) data using the standard algal_1 product. The satellite-retrieved Chl-*a* was fractionated into C_1 and $C_{2,3}$ using the model calibrated with the historic *in situ* dataset (Section 4.1.2.1).

4.1.3.1 Performance of MERIS Chl-a

MERIS Chl-*a* was validated against *in situ* Chl-*a*, which was a sum of the combined fractions (C_1+$C_{2,3}$). A range of published Chl-*a* algorithms were tested, including 2- and 3-band empirical models (Gitelson et al. 2008), the normalised difference chlorophyll index (NDCI; Mishra & Mishra, 2012), semi-analytical models (Gons et al., 2005) and the standard algal_1 and algal_2 MERIS products. The lowest errors for Chl-*a* retrieval using the MERIS L2 data were for the standard algal_1 product, therefore this Chl-*a* product was taken forward for application of the PSC model (Figure 9).

We note that the PSC model performance is highly dependent on a good Chl-*a* retrieval. Thus, this is a fundamental issue that also needs to be addressed for a Sentinel-3 PSC product, and these Chl-a and PSC validation results will be presented in the D3.8 Validation Report.

(a) (b) (c)

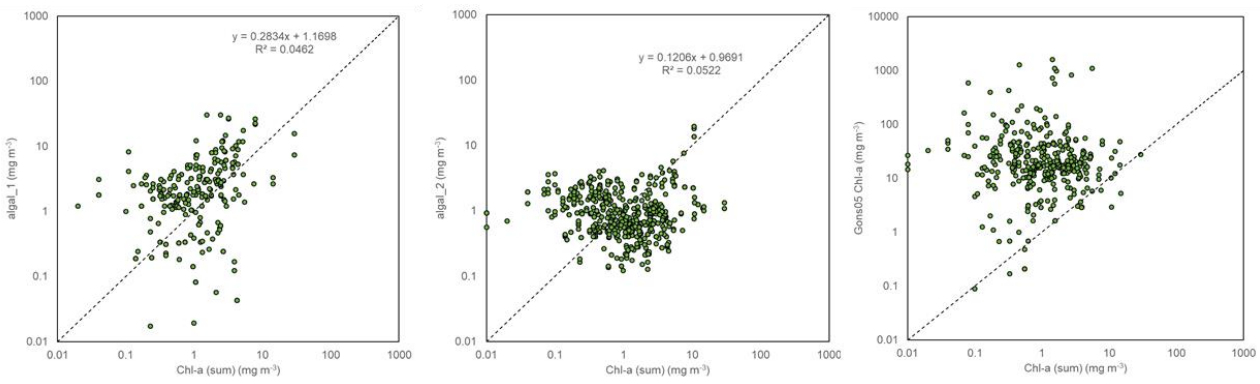

Figure 9 – Selected MERIS Chl-a retrieval validation results for (a) algal_1, (b) algal_2 and (c) Gons et al. 2005 (Gons05).

This project has received funding from the European Union's Horizon 2020 research and innovation programme under grant agreement No 776348

4.1.3.2 Performance of MERIS PSC

Validation results for the 2-class PSC model applied to MERIS Chl-*a* are shown below in Figure 10 and Figure 11. Example maps of PSC applied to MERIS are shown in Figure 12.

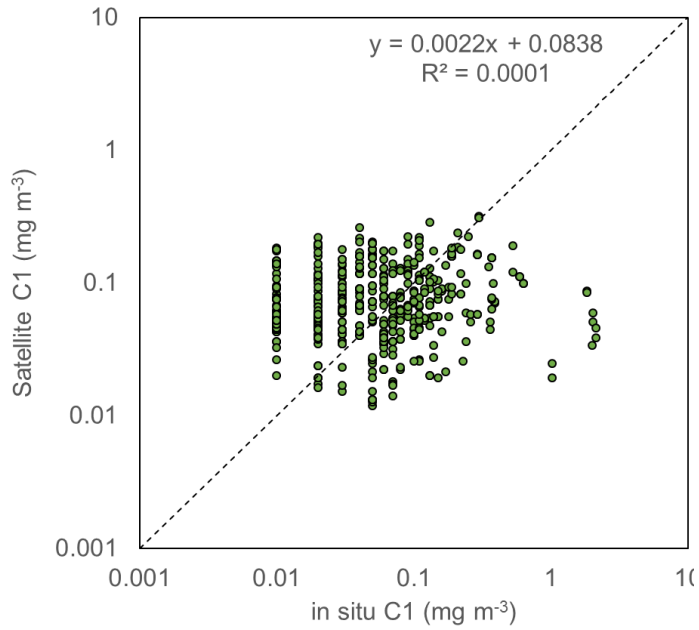

Error metric	Value
$RMSE_{log}$	0.531
MAE_{log}	0.422
MAPE	176%
$Bias_{log}$	-0.104

Figure 10 – Satellite model validation results for pico-phytoplankton ($C_1 = C_1^m[1 - exp(-S_1C)]$).

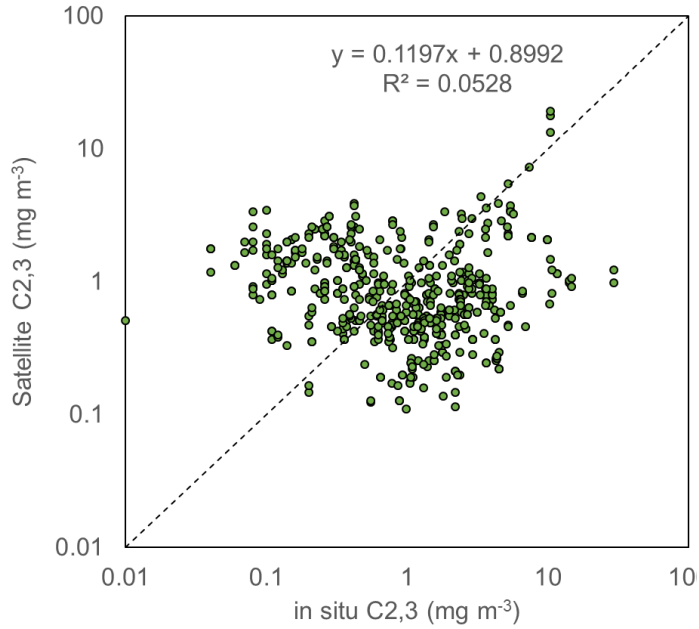

Error metric	Value
$RMSE_{log}$	0.662
MAE_{log}	0.551
MAPE	264%
$Bias_{log}$	0.0640

Figure 11 – Satellite model validation results for nano- + micro-phytoplankton ($C_{2,3} = C - C_1$).

This project has received funding from the European Union's Horizon 2020 research and innovation programme under grant agreement No 776348

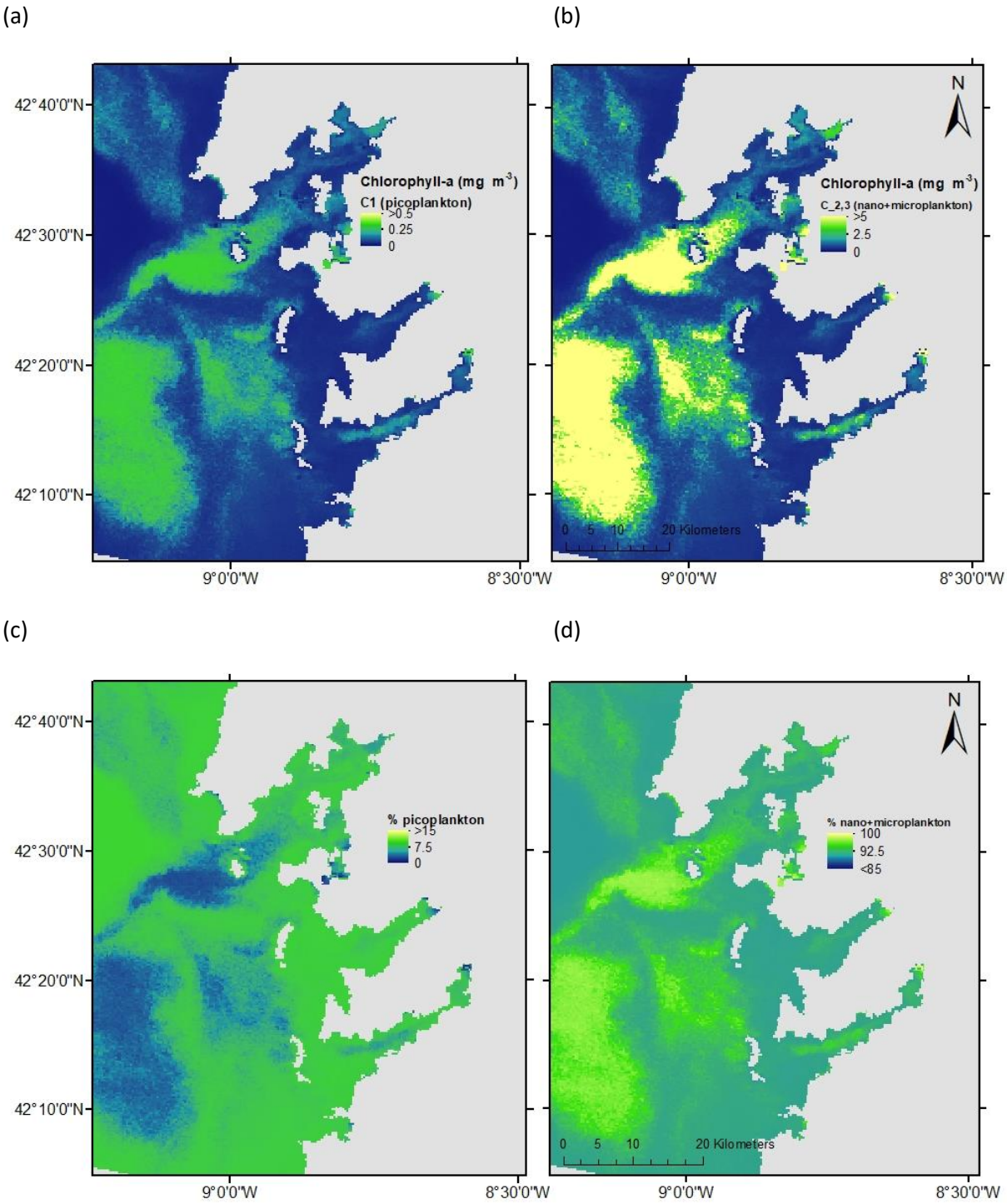

Figure 12 – Example maps of PSC using the 2-class model for MERIS in the Galician coastal waters of Spain (04 June 2006), including (a) concentration and (c) % of pico-phytoplankton (C_1), and (b) concentration and (d) % of nano- + micro-phytoplankton.

This project has received funding from the European Union's Horizon 2020 research and innovation programme under grant agreement No 776348

4.2 2018-2019 Dataset

Data were collected at three coastal sites as part of the 2018 CoastObs campaigns to support development of the PSC product (Table 3; Figure 13). Additionally, further campaigns are planned for 2019 to collect further validation data.

Table 3 – Summary of field campaigns completed and planned in support of PSC product validation (2018-2019)

Location	Samples collected	Campaign dates
Venice Lagoon and the Adriatic Sea (Italy)	Chl-*a* Fractionated Chl-*a* HPLC pigments Particulate absorption	2-8 May 2018 25-28 June 2018 15-28 July 2019 (planned)
Ria de Vigo (Spain)	Chl-*a* Fractionated Chl-*a* HPLC pigments Particulate absorption	30 May 2018 04-17 July 2018 01-22 June 2019 (planned)
Wadden Sea and the Eastern Scheldt (Netherlands)	Chl-*a* HPLC pigments	Weekly April – October 2018
	Chl-*a* Fractionated Chl-*a* HPLC pigments Particulate absorption	11-17 August 2019 (planned)

This project has received funding from the European Union's Horizon 2020 research and innovation programme under grant agreement No 776348

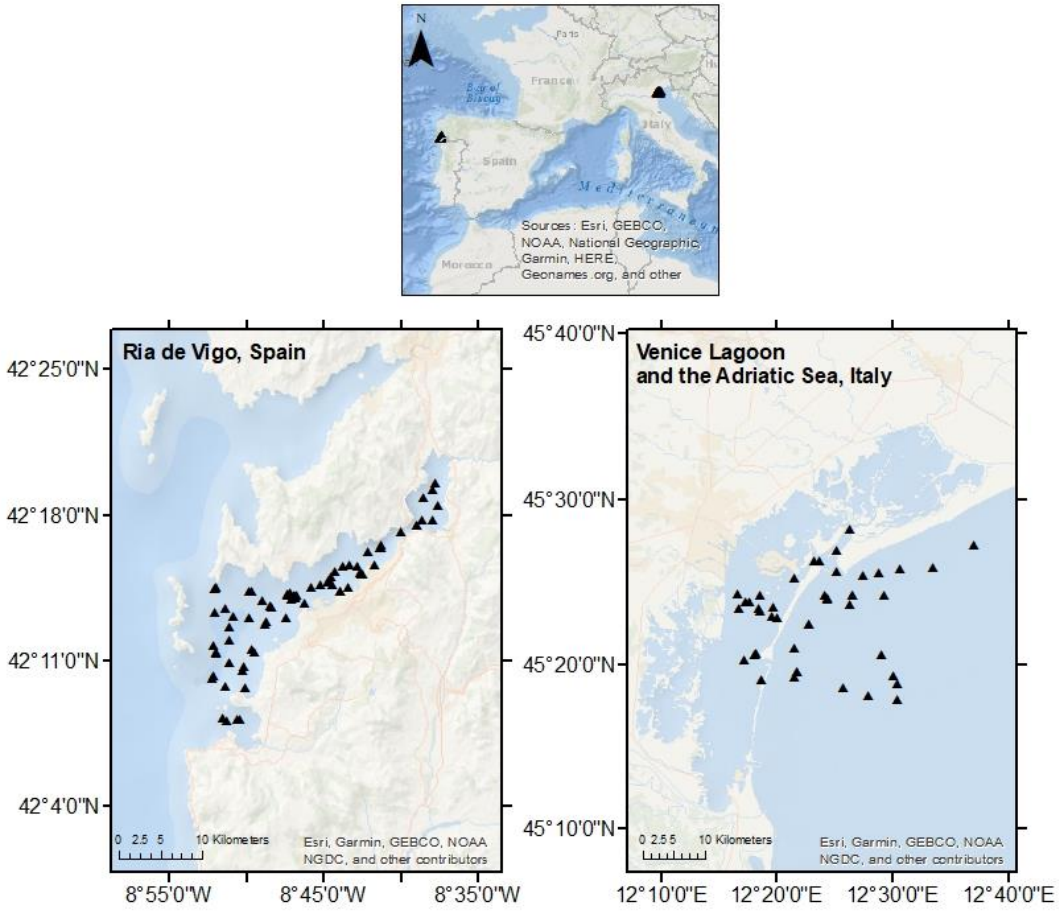

Figure 13 – Stations sampled in Ria de Vigo (Spain) and Venice Lagoon and the Adriatic Sea (Italy) in 2018 to support PSC product validation

4.2.1 Methods

4.2.1.1 In situ

Samples were collected from the surface and kept cool in the dark for filtration within 24 hours. For total pigment analysis, water samples were filtered through Whatman GF/F filter papers. For fractionated Chl-*a* and particulate absorption analysis, water samples were filtered through a series of three filter papers of 0.2, 2 and 20 µm pore sizes (GF/F and nucleopore). All filter papers were stored in cryovials at -80°C prior to analysis.

For analysis of Chl-*a* and accessory pigments, filter paper pigment was extracted in 3 ml of 100% HPLC grade methanol, according to the LOV method (Claustre and Ras, 2005). This included freezing at -20°C (minimum 30 min), sonication (duty cycle 50% at 10s), freezing again at -20°C (minimum 30 min), then clarification of each sample by syringe filtration. Finally, samples were analysed within 24 hours by High Performance Liquid Chromatography (HPLC).

This project has received funding from the European Union's Horizon 2020 research and innovation programme under grant agreement No 776348

Fractionated particulate absorption samples were analysed by dual beam spectrophotometry, following the method of Tassan and Ferrari (1995).

4.2.1.2 Model

Given the good performance of the abundance-based model with the historic dataset (using *in situ* data), this method was applied for the 2018 dataset.

Using the *in situ* fractionated Chl-*a* data from Venice and Vigo 2018 field campaigns, the 3-class model of Brewin et al. (2010) was applied. As in the original Brewin et al. (2010) model, total Chl-*a* (C) was a sum of the three fractions (Equation 1), where:

C_1 = Chl-*a* 0.2-2 µm (pico-phytoplankton)

C_2 = Chl-*a* 2-20 µm (nano-phytoplankton)

C_3 = Chl-*a* >20 µm (micro-phytoplankton)

4.2.2 Performance of Venice *in situ* model

For the Venice dataset only, both the pico-phytoplankton (C_1) and the combined pico- and nano-phytoplankton ($C_{1,2}$) were modelled according to an exponential function as in Brewin et al (2010) (Equations 2,3). Models for C_1 and $C_{1,2}$ were fitted using a standard nonlinear least squares method (Levenberg-Marquardt, R `minipack.lm` package).

C_2 was then calculated by subtraction (Equation 4), and micro-phytoplankton, C_3, was derived by subtraction of C1,2 from total Chl-*a*, C (Equation 5).

4.2.2.1 Retuned model parameters for C_1 (Pico-phytoplankton) and $C_{1,2}$ (Pico- + Nano-phytoplankton)

The model for C_1 is shown below, indicating an exponential decreasing model with high significance ($p<0.05$; Figure 14). $C_{1,2}$ was also modelled as an exponential decreasing function, however the coefficients were not significant ($p>1$; Figure 15). The coefficients for the models for C_1 and $C_{1,2}$ are shown in Table 4.

This project has received funding from the European Union's Horizon 2020 research and innovation programme under grant agreement No 776348

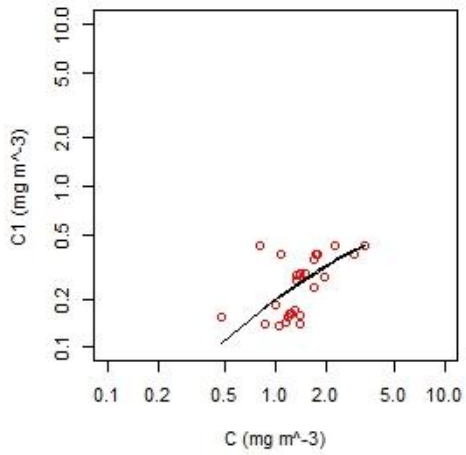

Figure 14 – In situ exponential model for fraction of Chl-a attributed to pico-phytoplankton (C_1) as a function of total Chl-a (C) ($C_1 = C_1^m[1 - exp(-S_1 C)]$, p<0.05).

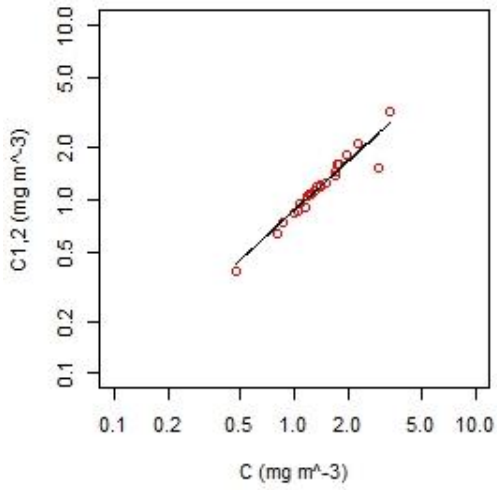

Figure 15 – In situ exponential model for fraction of Chl-a attributed to pico- + nano-phytoplankton ($C_{1,2}$) as a function of total Chl-a (C) ($C_{1,2} = C_{1,2}^m[1 - exp(-S_{1,2} C)]$; p>1).

Table 4 - Retuning coefficients for the Venice 3-class PSC model

Phytoplankton fraction	Coefficient	Value
Pico-phytoplankton (C_1)	C_1^m	0.5486
	S_1	0.4501
Pico- + nano-phytoplankton ($C_{1,2}$)	$C_{1,2}^m$	12.3
	$S_{1,2}$	0.0737

This project has received funding from the European Union's Horizon 2020 research and innovation programme under grant agreement No 776348

4.2.2.2 Model performance

The model was applied to *in situ* total Chl-*a* (C) to derive a modelled C_1 and $C_{1,2}$. From these, C_2 and C_3 were calculated by subtraction. The model validation plots are shown in Figure 16 and indicate fairly good agreement between modelled and measured values (R^2 = 0.29-0.80).

This project has received funding from the European Union's Horizon 2020 research and innovation programme under grant agreement No 776348

(a)

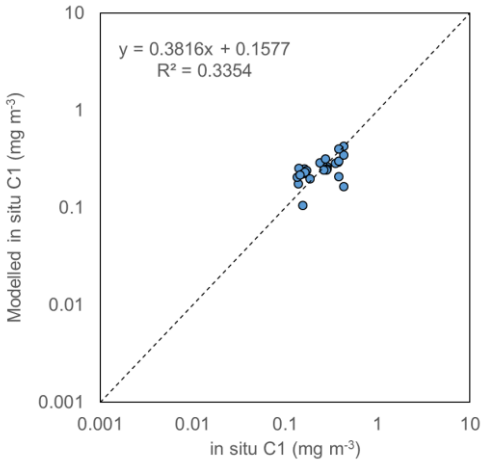

(b)

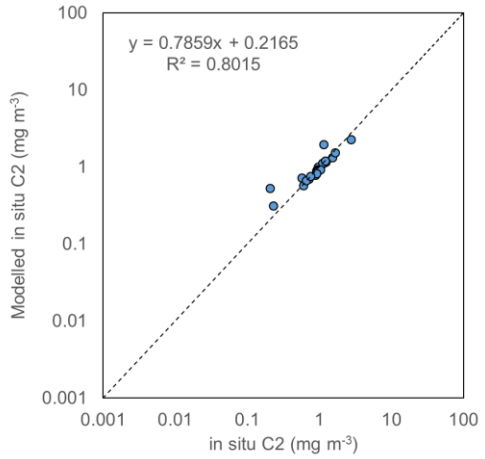

(c)

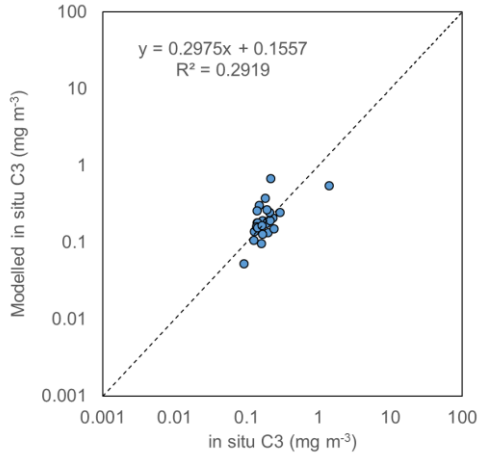

Figure 16 – In situ model performance for (a) pico-phytoplankton (C_1), (b) nano-phytoplankton (C_2) and (c) micro-phytoplankton (C_3).

This project has received funding from the European Union's Horizon 2020 research and innovation programme under grant agreement No 776348

4.2.3 Performance of Vigo *in situ* model

For the Vigo dataset only, the Chl-*a* concentration for the smallest size class (C_1) was frequently zero (i.e. no pico-phytoplankton were present). Secondly, it was observed that the largest size class (C_3) followed a decreasing exponential model (Figure 17). Therefore, the Brewin et al. (2010) model was adapted for Vigo as follows:

$$C_3 = C_3^m[1 - \exp(-S_3 C)] \quad (9)$$

$$C_{2,3} = C_{2,3}^m\left[1 - \exp(-S_{2,3} C)\right] \quad (10)$$

C_2 was then calculated by subtraction:

$$C_2 = C_{2,3} - C_3 \quad (11)$$

and pico-phytoplankton, C_1, was derived by subtraction of $C_{2,3}$ from total Chl-*a*, C:

$$C_1 = C - C_{2,3} \quad (12).$$

4.2.3.1 Retimed model parameters for C_3 (micro-phytoplankton) and $C_{2,3}$ (Pico- + Nano-phytoplankton)

The model for C_3 is shown below, indicating an nonlinear asymptotic model with high significance ($p<0.001$; Figure 17). In contrast to Venice, the micro-phytoplankton size class show an asymptotic pattern in the Vigo 2018 dataset. The theory is that in coastal waters with significant mussel aquaculture, there may be an upper limit imposed from the top-down (e.g. grazing) processes. Mussels filter feed preferentially for micro-phytoplankton, while the smaller phytoplankton size classes are not retained. Additionally, it may be that with the greater Chl-*a* concentration in Vigo coastal waters (~0.1-10 mg m^{-3}) the asymptotic feature can be observed for micro-phytoplankton, whereas this simply appears linear in waters with lower Chl-*a* (e.g. Venice Lagoon and Adriatic; ~0.5-5 mg m^{-3}) or open ocean (~0.001-1 mg m^{-3}). Therefore, this is likely a specific model for a case with a large fraction of micro-phytoplankton present, and where this class has an upper limit with increasing total Chl-*a*.

This project has received funding from the European Union's Horizon 2020 research and innovation programme under grant agreement No 776348

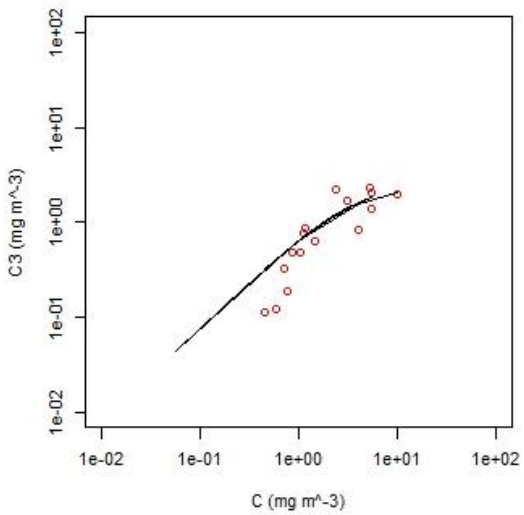

Figure 17 – In situ exponential model for fraction of Chl-a attributed to micro-phytoplankton (C_3) as a function of total Chl-a (C) ($C_3 = C_3^m[1 - exp(-S_3C)]$, p<0.001).

The model for $C_{2,3}$ is shown below, indicating an exponential model with high significance (p<0.01; Figure 18). The model coefficients for both C_3 and $C_{2,3}$ are shown in Table 5.

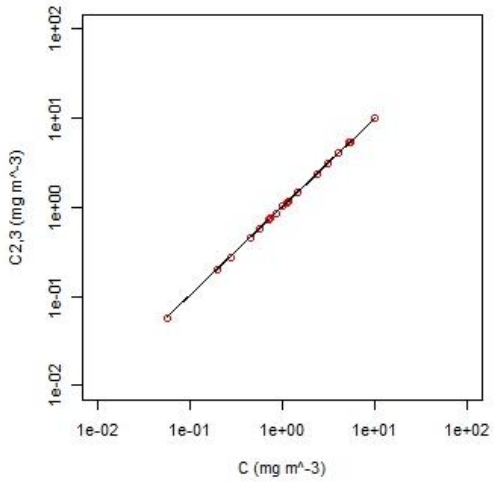

Figure 18 – In situ exponential model for fraction of Chl-a attributed to nano- + micro--phytoplankton ($C_{2,3}$) as a function of total Chl-a (C) ($C_{2,3} = C_{2,3}^m[1 - exp(-S_{2,3}C)]$, p<0.01).

This project has received funding from the European Union's Horizon 2020 research and innovation programme under grant agreement No 776348

Table 5 - Retuning coefficients for the Vigo 3-class PSC model

Phytoplankton fraction	Coefficient	Value
Micro-phytoplankton (C_3)	C_3^m	2.1219
	S_3	0.3596
Nano- + nano-phytoplankton ($C_{2,3}$)	$C_{2,3}^m$	164.8
	$S_{2,3}$	0.00619

4.2.3.2 Model performance

The model was applied to *in situ* total Chl-*a* (C) to derive a modelled C_3 and $C_{2,3}$. From these, C_1 and C_2 were calculated by subtraction. The model validation plots are shown in Figure 19and indicate good agreement between modelled and measured values (R^2 = 0.79-0.96).

This project has received funding from the European Union's Horizon 2020 research and innovation programme under grant agreement No 776348

(a)

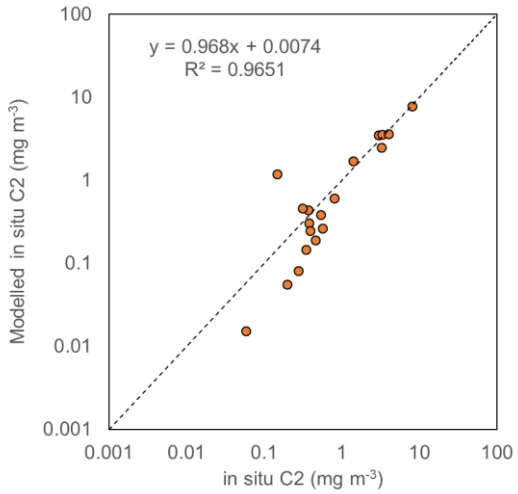

(b)

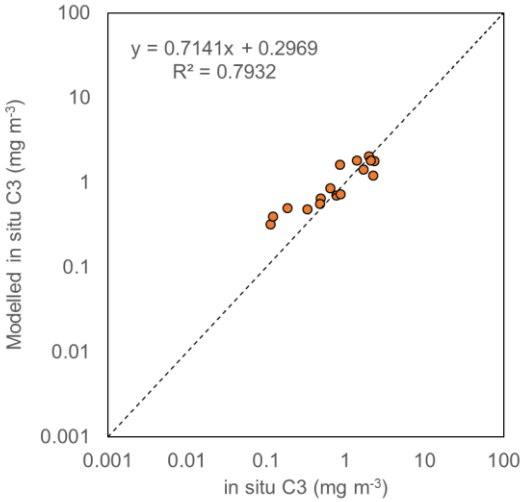

Figure 19 – In situ model performance for (a) nano-phytoplankton (C_2) and (b) micro-phytoplankton (C_3). Not shown: pico-phytoplankton (C_1) performance, as there was only one matchup with a non-zero in situ C_1.

4.2.4 Performance of satellite model

The PSC 3-class model will be forced with satellite Chl-*a* from Sentinel-2 and -3, and validated with the *in situ* fractionated Chl-*a* from the 2018 and 2019 field campaigns. These results will be provided in the Final Validation Report (D 3.8).

This project has received funding from the European Union's Horizon 2020 research and innovation programme under grant agreement No 776348

5 Conclusions and future work

Future work will include validation of the models for PSC from Sentinel-3 OLCI and Sentinel-2 MSI data using the 2019 field campaign data for fractionated Chl-*a*, pigments (by HPLC) and fractionated absorption. Field campaigns are planned to collect these data in the coastal waters of Venice, Vigo and the Netherlands over summer 2019. These validation results will be presented in the Validation Report (D3.8).

The results are promising for the abundance-based PSC approach, using a site specific 3-class model. However, future work will include testing of the pigment- and absorption-based based models using the Vigo, Venice and Netherlands datasets (2018-19) once the data analysis for these samples is complete.

This project has received funding from the European Union's Horizon 2020 research and innovation programme under grant agreement No 776348

6 References

Barnes, C., Irigoien, X., De Oliveira, J.A., Maxwell, D., Jennings, S. (2011) Predicting marine phytoplankton community size structure from empirical relationships with remotely sensed variables. J. Plankton Res., 33: 13–24.

Brewin, R.J.W., Sathyendranath, S., Hirata, T., Lavender, S.J. Barciela, R.M., Hardman-Mountford, N.J. (2010) A three-component model of phytoplankton size class for the Atlantic Ocean. Ecological Modelling, 221: 1472-1483.

Brewin, R.J.W., Ciavatta, S., Sathyendranath, S., Jackson, T., Tilstone, G., Curran, K., Airs, R.L., Cummings, D., Brotas, V., Organelli, E., Dall'Olmo, G., Raitsos, D.E. (2017) Uncertainty in Ocean-Color Estimates of Chlorophyll for Phytoplankton Groups. Frontiers in Marine Science, 4(104): 1-22.

Bricaud, A., Babin, M., Morel, A., Claustre, H. (1995) Variability in the chlorophyll-specific absorption coefficients of natural phytoplankton: Analysis and parameterization. Journal of geophysical research, 100 (C7): 13321-13332.

Caddy, J.F., Fefk, R., Do-Chi, T. (1995) Productivity estimates for the Mediterranean: evidence of accelerating ecological change. Effects of riverine inputs on coastal ecosystems and fisheries resources. *FAO Tech*. Rep 249, 1–17. FAO, Rome.

Chisholm, S.W. (1992). *Phytoplankton size.* In: Falkowski, P.G., Woodhead, A.D. (Eds.), Primary Productivity and Biogeochemical Cycles in the Sea. Springer, New York, pp. 213–237.

Claustre, H. and Ras, J. (2005). *Chapter 6: The LOV Method* in The Second SeaWiFS HPLC Analysis Round-Robin Experiment (SeaHARRE-2), NASA, Maryland.

Devred, E., Sathyendranath, S., Stuart, V., Maas, H., Ulloa, O., Platt, T. (2006) A two component model of phytoplankton absorption in the open ocean: theory and applications. *Journal of Geophysical Research*, 111: C03011.

Finkel, Z.V.; Beardall, J.; Flynn, K.J.; Quigg, A.; Rees, T.A.V.; Raven, J.A. (2009) Phytoplankton in a changing world: Cell size and elemental stoichiometry. *J. Plankton Res.* 32: 119–137.

Gitelson, A., Dall'Olmo, G., Moses, W.J., Rundquist, D.C., Barrow, T.M., Simon, T., Fisher, R., Gurlin, D., Holz, J.C. (2008) A simple semi-analytical model for remote estimation of chlorophyll-*a* in turbid waters: Validation. *Remote Sensing of Environment*, 112: 3582–3593, doi:10.1016/j.rse.2008.04.015.

Gons, H., Rijkeboer, M., Ruddick, K.G. (2005) Effect of a waveband shift on chlorophyll retrieval from MERIS imagery of inland and coastal waters. Journal of Plankton Research, 27(1): 125-127.

This project has received funding from the European Union's Horizon 2020 research and innovation programme under grant agreement No 776348

Hirata, T., Aiken, J., Hardman-Mountford, N.J., Smyth, T.J., Barlow, R.G. (2008) An absorption model to derive phytoplankton size classes from satellite ocean colour. *Remote Sensing of Environment*, 112(6): 3153-3159.

Irwin, A.J. (2006) Scaling-up from nutrient physiology to the size-structure of phytoplankton communities. *J. Plankton Res.* 28: 459–471.

Jørgensen, C.B. (1990) Functional morphology of bivalve feeding. *In* Bivalve Filter Feeding: Hydrodynamics, Bioenergetics, Physiology and Ecology, Olsen & Olsen, Fredensborg, pp. 4-10.

Liu, X., Devred, E., Johnson, C. (2018) Remote Sensing of Phytoplankton Size Class in Northwest Atlantic from 1998 to 2016: Bio-Optical Algorithms Comparison and Application. *Remote Sensing*, 10(7): 1028. https://doi.org/10.3390/rs10071028

Marañón, E. (2015) Cell size as a key determinant of phytoplankton metabolism and community structure. *Annu. Rev. Mar. Sci.*, 7: 241–264.

Mishra, S. and Mishra, D. (2012) Normalized difference chlorophyll index: A novel model for remote estimation of chlorophyll-*a* concentration in turbid productive waters. *Remote Sensing of Environment*, 117: 394-406.

Møhlenberg, F. and Riisgård, H.U. (1978) Efficiency of particle retention in 13 species of suspension feeding bivalves. *Ophelia*, 17(2): 239-246.

Muñiz, O., Revilla, M., Rodríguez, J.G., Laza-Martínez, A. Fontán, A. (2019) Annual cycle of phytoplankton community through the water column: Study applied to the implementation of bivalve offshore aquaculture in the southeastern Bay of Biscay. *Oceanologia*, 61(1): 114-130.

Nair, A.; Sathyendranath, S.; Platt, T.; Morales, J.; Stuart, V.; Forget, M.-H.; Devred, E.; Bouman, H. (2008) Remote sensing of phytoplankton functional types. *Remote Sens. Environ*. 112: 3366–3375.

Neveaux, J. and Panouse, M. (1987) Spectrofluorometric determination of chlorophylls and pheophytins. *Arch Hydrobiol*. 109: 567-581.

Parsons, T.R., Lalli, C.M. (2002) Jellyfish populations explosions: revisiting a hypothesis of possible causes. *La Mer,* 40: 111–121.

Platt, T., Denman, K.L. (1976) The relationship between photosynthesis and light for natural assemblages of coastal marine phytoplankton. *Journal of Phycology*, 12(4): 421–430.

Platt, T., Denman, K.L. (1977) Organisation in the pelagic ecosystem. *Helgoa Ender Wissenschaftliche Meeresuntersuchungen,* 30: 575–581.

This project has received funding from the European Union's Horizon 2020 research and innovation programme under grant agreement No 776348

Platt, T., Denman, K.L. (1978) The structure of pelagic marine ecosystems. Rapp. P. -v. Réun. Cons. perm. int. Explor. *Mer*, 60–65.

Raven, J.A. (1998) Small is beautiful: the picophytoplankton. *Functional Ecology,* 12: 503–513.

Riisgård, HU. (1988) Efficiency of particle retention and filtration rate in 6 species of Northeast American bivalves. *Marine Ecological Progress Series*, 45: 217-223.

Safi, K.A. and Gibbs, M.M. (2003) Importance of different size classes of phytoplankton in Beatrix Bay, Marlborough Sounds, New Zealand, and the potential implications for the aquaculture of the mussel, Perna canaliculus. New Zealand Journal of Marine and Freshwater Research, 37(2): 267-272.

Sathyendranath, S., Stuart, V., Cota, G., Maas, H., Platt, T. (2001) Remote sensing of phytoplankton pigments: a comparison of empirical and theoretical approaches. International Journal of Remote Sensing, 22: 249-273.

Sieburth, J.M.; Smetacek, V.; Lenz, J. (1978) Pelagic ecosystem structure: Heterotrophic compartments of the plankton and their relationship to plankton size fractions. *Limnol. Oceanogr.* 23: 1256–1263.

Sonier, R., Filgueira, R. , Guyondet, T., Tremblay, R., Olivier, F., Meziane, T., Starr, M., LeBlanc, A. R., and Comeau, L. A. (2016) Picophytoplankton contribution to *Mytilus edulis* growth in an intensive culture environment, *Marine Biology,* 163: 73. https://doi.org/10.1007/s00227-016-2845-7

Tassan S., and Ferrari G.M., (1995) An alternative approach to absorption measurements of aquatic particles retained on filters. Limnol. Oceanogr. 40: 1358-1368.

Uitz, J., Claustre, H., Morel, A., Hooker, S.B. (2006) Vertical distribution of phytoplankton communities in open ocean: an assessment based on surface chlorophyll. *Journal of Geophysical Research*, 111: CO8005.

Vidussi, F., H. Claustre, B. B. Manca, A. Luchetta, and J. C. Marty (2001). Phytoplankton pigment distribution in relation to upper thermocline circulation in the eastern Mediterranean Sea during winter, *J. Geophys. Res.,* 106(C9), 19,939–19,956.

Zapata, M., Ayala, A.M., Franco, J.M., Garrido, J.L. (1987) Separation of chlorophylls and their degredation products in marine-phytoplankton by reversed-phase high-performance liquid chromatography. *Chromatographia*, 23(1): 26-30.

This project has received funding from the European Union's Horizon 2020 research and innovation programme under grant agreement No 776348